
Deep Reinforcement Learning for Energy Management in Residential Housing

Tim Walter¹

Abstract

This paper provides a novel formulation of the problem of carbon intensity minimization in a smart home environment. The environment includes an energy storage system, a heat pump, and a flexible demand. The environment is formulated as a Markov Decision Process and tested using state of the art reinforcement learning methods. The effectiveness of the algorithms is compared to rule-based controllers. To improve performance three hypotheses and accompanying modifications were explored in an effort to aid the learning process.

1. Introduction

The operations of buildings account for 30% of global final energy consumption and 26 % of global energy-related greenhouse-gas emissions (IEA, 06.01.2024). This makes the optimization of energy consumption a major concern for environmental sustainability. This paper investigates the application of Deep Reinforcement Learning (DRL) to streamline energy usage within a single-family home, leveraging solar panels, electric batteries, heat pumps, and flexible demand mechanisms. The primary aim is to reduce the carbon footprint associated with housing operations.

2. Related Work

The application field of smart energy management encompasses a wide range of problems, such as heating and cooling (Blum et al., 2021)(Thomas Schreiber et al., 2020), flexible demand response (Jin et al., 2021) and energy storage (Nakabi & Toivanen, 2021). Moreover, the scale and level of detail of the tackled problems vary greatly, going from single buildings (Blum et al., 2021), to microgrids (Nakabi & Toivanen, 2021) (Castellanos et al.)

to eventually continent-wide electricity grids (Hörsch et al., 2018). The two most promising approaches to solve such problems are classical Model Predictive Control (MPC) (Basantes et al., 2023) and Reinforcement Learning (RL) (Nakabi & Toivanen, 2021) (Jin et al., 2021) (Thomas Schreiber et al., 2020)(Zhu et al., 2022). Furthermore, there are also hybrid approaches that combine the two methods (Javier Arroyo et al., 2022).

This paper is mainly inspired by (Nakabi & Toivanen, 2021), who describe a microgrid environment with generation, storage and consumers and optimized electricity pricing using various deep reinforcement learning algorithms.

3. Environment

The main contribution of this work is an environment for a single-family household, consisting of a Rooftop Solar Array (RSA), an Energy Storage System (ESS), a Thermostatically Controlled Load (TCL) and Flexible Demand Response (FDR). The environment is a mixture of replayed data and dynamic components. The objective is minimizing the CO₂eq emissions. The environment is built on the Gymnasium framework (Towers et al., 2023) and available on GitHub¹. The task is split into episodes of weeks, with either minutely or hourly resolution, to capture the daily and weekly patterns of the demand and generation.

The RL paradigm requires the formulation as a Markov Decision Process, consisting of a transition function, action and observation spaces, and a reward function. The transition function is given by the replayed data and the dynamics of the components in the following. The observation space is a bounded subset of \mathbb{R}^{11+H} , with the observables given in Table 1. The action space is summarized in Table 2. The reward function is described in Section 3.5.

3.1. Replayed Data

The data was either given in hourly or minutely resolution, and was adapted to the missing resolution using linear interpolation or averaging. The most relevant observables are displayed exemplary in Figure 1.

¹Department of Scientific Computing, Technical University of Munich, Munich, Germany. Correspondence to: Tim Walter <tim.walter@tum.de>.

¹<https://github.com/TimWalter/smart-energy-controller>

The auxiliary information included weather and time data, which provided means for the agent to predict the carbon intensity of the electricity mix and the heating demand. It was sourced from the Photovoltaic Geographical Information System (PVGIS) (Thomas Huld et al., 2012).

The RSA was simulated using the PVLIB library (F. Holmgren et al., 2018), with panel specifications from the CEC database (Dobos, 2012)(Boyson et al., 2007).

The household's energy demand was sourced from the UCI archive (Georges Hebrail). Since the consumption was unraveled for different rooms, the kitchen, electric water heater and air conditioner were modeled as inflexible demand, while the laundry room as flexible demand.

The direct carbon intensity of the electricity mix at any given time was sourced from Electricity Maps (Ele, 29.12.2023).

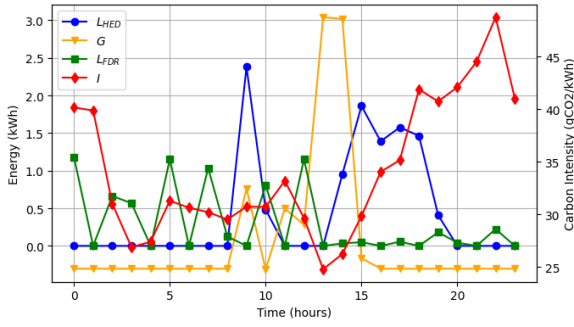


Figure 1. Replayed data for the first 24 hours.

3.2. Energy Storage System

The ESS is connected to the grid and the RSA. The charge is subject to the following dynamics

$$B_t = \max\{0, B_{t-1} - D_s + C_t\sqrt{\nu} - \frac{D_t}{\sqrt{\nu}}\}. \quad (1)$$

Here, $B_t \in [0, B_{max}]$ is the charge at time t and B_{max} is the capacity. Furthermore, ν denotes the round trip efficiency, D_s the self-discharge rate, $C_t \in [0, C_{max}]$ the charge rate with maximum C_{max} and $D_t \in [0, D_{max}]$ the discharge rate with its maximum D_{max} .

3.3. Flexible Demand Response

The FDR can be influenced stochastically in a running time window of length H by a signal $a_{fdr,t} \in [-1, 1]^H$. Whether the power is consumed is determined by a Bernoulli process, with probabilities

$$p_t = \text{clip}\left(s + a_{fdr,t} * \exp\left(\frac{-1}{\beta} |t - t_s|\right), 0, 1\right), \quad (2)$$

where $s \in \{0, 1\}^H$ indicates the desired consumption with elements $s_i = \begin{cases} 1 & \text{if } t_i \leq t \\ 0 & \text{else,} \end{cases}$ β is a patience parameter, and

$t_s \in \mathbb{R}^H$ is the desired consumption time. If consumption is delayed more than once, $\frac{2}{H-1}$ of the power is consumed in each time step to ensure that all power has been consumed after the time window. This aims to facilitate learning by preventing infinite delays or a large correction at episode termination.

3.4. Thermostatically Controlled Load

The TCL encapsulates all devices that aim to maintain the temperature of a given heat mass. To utilize such loads as energy storage, the temperature of the heat mass is allowed to fluctuate within a given range. The TCL is modeled as a second-order system (Sonderegger, 1978) with the following dynamics:

$$\begin{aligned} T_t = & T_{t-1} + \frac{1}{r_a}(T_{a,t} - T_{t-1}) \\ & + \frac{1}{r_b}(T_{b,t} - T_{t-1}) \\ & + \frac{1}{r_h}L_{TCL}a_{tcl,t} + q \end{aligned} \quad (3)$$

, where T is the indoor temperature, r_a is the thermal mass of the air, T_a is the outdoor temperature, r_b is the thermal mass of the building material, and T_b is the building mass temperature, that evolves with

$$T_{b,t} = T_{b,t-1} + \frac{1}{r_b}(T_{t-1} - T_{b,t-1}), \quad (4)$$

, $\frac{1}{r_h}$ is the power-to-heat coefficient, L_{TCL} is the nominal power, $a_{tcl,t} \in [-1, 1]$ is the heating signal, and q is the unintentional heat drift. The heating signal is constrained by the desired temperature range, enforced through a backup controller as follows:

$$a_{tcl,t} = \begin{cases} -1 & \text{if } T_t \geq T_{max} \\ 1 & \text{if } T_t \leq T_{min} \\ a_{tcl,t} & \text{else} \end{cases} \quad (5)$$

, where T_{max} and T_{min} define the desired temperature range.

3.5. Reward Function

The given objective of minimizing CO2eq emission is augmented by a temperature discomfort penalty to avoid unintended exploitation of the TCL, which is often optimal

Table 1. Observation Space.

OBSERVABLE	SYMBOL	REPLAYED
CARBON INTENSITY	I	X
HOUSEHOLD ENERGY DEMAND	L_{HED}	X
ROOFTOP SOLAR GENERATION	G	X
ESS CHARGE	B	
FDR POWER IN WINDOW	L_{FDR}	
INDOOR TEMPERATURE	T	
TIME STEP	t	X
MONTH OF YEAR	MoY	X
SOLAR IRRADIATION	SI	X
SOLAR ELEVATION	SE	X
OUTDOOR TEMPERATURE	T_a	X
WIND SPEED	WS	X

Table 2. Action Space.

ACTION	MIN. MEANING	MAX. MEANING
a_{ess}	DISCHARGE	CHARGE
a_{fdr}	DELAY	EXPEDITE
a_{tcl}	NO HEATING	HEATING

at constant T_{min} . The resulting reward function is

$$r_t = I_t(PE - CE) - DC \quad (6)$$

$$E_C = L_t + \frac{1}{r_h} L_{TCL} a_{tcl,t} + C_t + \sum_{p \in U_e} p_r + \sum_{p \in U_d} \frac{2p}{H-1} \quad (7)$$

$$E_p = G_t + D_t \quad (8)$$

$$DC = \delta \exp(|T_t - \frac{T_{max} + T_{min}}{2}|) \quad (9)$$

where U_e is the set of consumed FDR, p_r is the remaining power after discounting, U_d is the set of delayed FDR, and δ the discomfort coefficient.

Since the task is episodic, it necessitates a correction at termination to evaluate the remaining state. The terminal reward is corrected by

$$reward += I_t B_t \quad (10)$$

$$reward += I_t (-\sum_{p \in U} p_r) \quad (11)$$

$$reward += I_t (-r_h |T_t - \frac{T_{max} + T_{min}}{2}|) \quad (12)$$

where U is the set of remaining FDR.

4. Experiments

As non-learning baselines an idle policy, which would always return zero actions, whose cumulative reward in

the first episode is shown in Figure 2, and a thresholding policy, see Appendix B, were implemented.

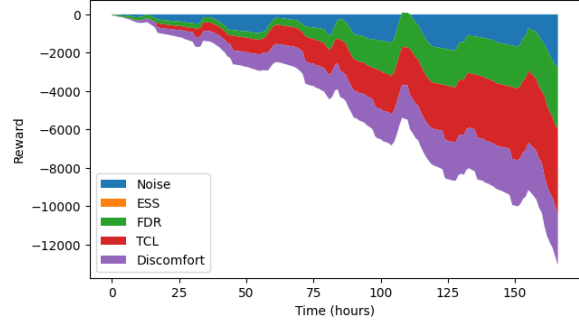


Figure 2. Cumulative reward for the idle policy.

As learning agents, Soft Actor Critic (SAC) (Haarnoja et al.) and Proximal Policy Optimization (PPO) (Schulman et al.) were chosen. Both implementations were taken from stable baselines 3 (Antonin Raffin et al., 2021), for details see Appendix C and Appendix D.

To allow for differentiation on which sub-tasks the agent performs well, the reward was split by the component of origin, as in Appendix F.

The results of all experiments are shown in Table 3. Since the initial task did not yield reward convergence surpassing the baselines, as shown in Figure 3, three hypotheses with accompanying modifications to the environment were tested. The changes were cumulative and further details can be found in Appendix E.

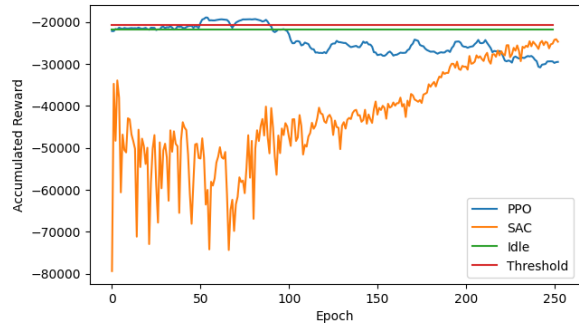


Figure 3. Training curve of the Full Environment.

4.1. Hypothesis 1: Scheduling, Stochasticity, and Dimensionality

The inherent scheduling challenge in the FDR sub-task is further exacerbated by the introduction of stochastic control. Furthermore, it bloats the dimensionality of the spaces with decreasing resolution, since the time window was fixed at 24 hours.

Table 3. Accumulated rewards split by origin per experiment. Evaluation was done after every epoch and the best result is shown.

EXPERIMENT	ALGORITHM	ESS	FDR	TCL	DISCOMFORT	TOTAL
FULL ENVIRONMENT	IDLE	0.00	-3173.56	-9887.61	-5912.63	-18973.80
	THRESHOLD	633.24	-3071.35	-9957.07	-5557.23	-17952.41
	PPO	0.00	-3233.98	-10825.89	-788.15	-14847.02
	SAC	60.24	-3087.39	-14692.60	-1637.00	-19356.75
HYPOTHESIS 1	IDLE	0.00	-3173.56	-9887.61	-5912.63	-18973.80
	THRESHOLD	633.24	-3068.56	-9957.07	-5557.23	-17949.62
	PPO	0.00	-3151.34	-11058.75	-531.89	-14741.98
	SAC	-40.18	-3192.11	-14329.95	-1258.60	-19820.84
HYPOTHESIS 2	IDLE	0.00	-3173.56	-9887.61	-5912.63	-18973.80
	THRESHOLD	633.24	-3068.56	-9957.07	-5557.23	-17949.62
	PPO	488.58	-3035.30	-10755.65	-3152.03	-14454.40
	SAC	157.94	-2969.78	-10114.51	-4906.66	-17832.01
HYPOTHESIS 3	IDLE	0.00	-3173.56	-9887.61	-5912.63	-18973.80
	THRESHOLD	633.24	-3068.56	-9957.07	-5557.23	-17949.62
	PPO	650.49	-3170.04	-10512.15	-5913.87	-18945.57
	SAC	599.65	-2969.36	-52971.76	-13164.96	-67506.43

To ease those challenges the control was changed to deterministic and scalar, and the observation to include only the sum of the time window. These changes are equivalent to the assumption that the optimal policy is invariant to U_e as long as the sum is maintained and that $\beta = \infty$.

The modified task only showed improvements for the minutely resolution, which suggests that high dimensionality is a problem. However, since convergence was still absent, the inefficiency of the other changes could not be concluded with certainty.

4.2. Hypothesis 2: Hard Exploration

The environment still provides a vast exploration space, due to the continuity of the spaces and the length of the episodes. Moreover, there is significant noise from the RSA and fixed demand on the reward. Moreover, a lot of observables are only relevant for estimating the future carbon intensity.

To address this the minutely resolution was omitted, the action space for PPO was discretised, the fixed demand and RSA were removed from the observables and reward calculation, and the agents were trained separately for each sub-task. Lastly, the replay buffer for SAC was initialized with transitions of the threshold algorithm, providing a warm start (Wang et al.).

The result indicated, that the discretisation aided PPO in learning the ESS but hindered in the TCL sub-task, hinting at a too coarse discretisation. SAC did not benefit from the warm start after a few epochs.

4.3. Hypothesis 3: Delayed or Deceptive reward

Another challenge of the setting is the reward structure for charging the ESS, expediting the FDR and heating or cooling the TCL. The rewards of those actions always occur delayed and only if the respective counter action is performed at a higher carbon intensity, which can be problematic. Moreover, the rewards might even be deceptive, since those actions are necessary for an effective policy but always yield immediate negative reward.

To test the hypothesis, the reward was transferred to an accumulating observable and only actuated in the terminal state, which should encourage the agent to evaluate the entire trajectory of an episode holistically.

Since the task was hardened by this change performance was expectedly decreased for TCL and FDR. However, the ESS sub-task showed signs of improvements but no convergence within the 250 training epochs.

5. Discussion

This paper provides an open challenge with a novel formulation of the problem of carbon intensity minimization in a smart home environment. Various experiments were run to test hypothesis on the cause of the learning inefficiency. While no single hypothesis led to a complete solution, two out of three aided the learning of some sub-tasks. A promising future direction would be to combine the various policies into an ensemble, with each controlling one subsystem.

References

- Electricity maps — reduce carbon emissions with actionable electricity data, 29.12.2023. URL <https://www.electricitymaps.com/>.
- Antonin Raffin, Ashley Hill, Adam Gleave, Anssi Kanervisto, Maximilian Ernestus, and Noah Dormann. Stable-baselines3: Reliable reinforcement learning implementations. *Journal of Machine Learning Research*, 22(268):1–8, 2021. URL <http://jmlr.org/papers/v22/20-1364.html>.
- Basantes, J. A., Paredes, D. E., Llanos, J. R., Ortiz, D. E., and Burgos, C. D. Energy management system (ems) based on model predictive control (mpc) for an isolated dc microgrid. *Energies*, 16(6):2912, 2023. doi: 10.3390/en16062912.
- Blum, D., Arroyo, J., Huang, S., Drgoňa, J., Jorissen, F., Walnum, H. T., Chen, Y., Benne, K., Vrabie, D., Wetter, M., and Helsen, L. Building optimization testing framework (bopstest) for simulation-based benchmarking of control strategies in buildings. *Journal of Building Performance Simulation*, 14(5):586–610, 2021. ISSN 1940-1493. doi: 10.1080/19401493.2021.1986574.
- Boyson, W. E., Galbraith, G. M., King, D. L., and Gonzalez, S. Performance model for grid-connected photovoltaic inverters. 2007. doi: 10.2172/920449. URL <https://www.osti.gov/biblio/920449>, journal=.
- Castellanos, J., Correa-Florez, C. A., Garcés, A., Ordóñez-Plata, G., Uribe, C. A., and Patino, D. An energy management system model with power quality constraints for unbalanced multi-microgrids interacting in a local energy market. URL <http://arxiv.org/pdf/2212.01910.pdf>.
- Dobos, A. P. An improved coefficient calculator for the california energy commission 6 parameter photovoltaic module model. *Journal of Solar Energy Engineering*, 134(2), 2012. ISSN 0199-6231. doi: 10.1115/1.4005759.
- F. Holmgren, W. W. Hansen, C., and A. Mikofski, M. pylib python: a python package for modeling solar energy systems. *Journal of Open Source Software*, 3(29):884, 2018. doi: 10.21105/joss.00884.
- Georges Hebrail, A. B. Individual household electric power consumption.
- Haarnoja, T., Zhou, A., Abbeel, P., and Levine, S. Soft actor-critic: Off-policy maximum entropy deep reinforcement learning with a stochastic actor. URL <http://arxiv.org/pdf/1801.01290.pdf>.
- Hörsch, J., Hofmann, F., Schlachtberger, D., and Brown, T. Pypsa-eur: An open optimisation model of the european transmission system. *Energy Strategy Reviews*, 22:207–215, 2018. ISSN 2211467X. doi: 10.1016/j.esr.2018.08.012. URL <http://arxiv.org/pdf/1806.01613.pdf>.
- IEA. Buildings - energy system - ie, 06.01.2024. URL <https://www.iea.org/energy-system/buildings>.
- Javier Arroyo, Carlo Manna, Fred Spiessens, and Lieve Helsen. Reinforced model predictive control (rl-mpc) for building energy management. *Applied Energy*, 309:118346, 2022. ISSN 0306-2619. doi: 10.1016/j.apenergy.2021.118346. URL <https://www.sciencedirect.com/science/article/pii/S0306261921015932>.
- Jin, L., Chen, Z., Li, J., and Ye, T. Reinforcement learning method based load shifting strategy with demand response. In *2021 40th Chinese Control Conference (CCC)*, pp. 1586–1591, 2021. doi: 10.23919/CCC52363.2021.9549975.
- Nakabi, T. A. and Toivanen, P. Deep reinforcement learning for energy management in a microgrid with flexible demand. *Sustainable Energy, Grids and Networks*, 25: 100413, 2021. ISSN 23524677. doi: 10.1016/j.segan.2020.100413.
- Schulman, J., Wolski, F., Dhariwal, P., Radford, A., and Klimov, O. Proximal policy optimization algorithms. URL <http://arxiv.org/pdf/1707.06347.pdf>.
- Sonderegger, R. C. *Dynamic models of house heating based on equivalent thermal parameters*. PhD thesis, Princeton University, New Jersey, 1978.
- Thomas Huld, Richard Müller, and Attilio Gambardella. A new solar radiation database for estimating pv performance in europe and africa. *Solar Energy*, 86(6):1803–1815, 2012. ISSN 0038-092X. doi: 10.1016/j.solener.2012.03.006. URL <https://www.sciencedirect.com/science/article/pii/S0038092X12001119>.
- Thomas Schreiber, Sören Eschweiler, Marc Baranski, and Dirk Müller. Application of two promising reinforcement learning algorithms for load shifting in a cooling supply system. *Energy and Buildings*, 229:110490, 2020. ISSN 0378-7788. doi: 10.1016/j.enbuild.2020.110490. URL <https://www.sciencedirect.com/science/article/pii/S0378778820320922>.

Towers, M., Terry, J. K., Kwiatkowski, A., Balis, J. U., de Cola, G., Deleu, T., Goulão, M., Kallinteris, A., KG, Arjun, Krimmel, M., Perez-Vicente, R., Pierré, A., Schulhoff, S., Tai, J. J., Shen, A. T. J., and Younis, O. G. Gymnasium, 2023. URL <https://zenodo.org/record/8127025>.

Wang, H., Lin, S., and Zhang, J. Warm-start actor-critic: From approximation error to sub-optimality gap. URL <http://arxiv.org/pdf/2306.11271.pdf>.

Zhu, D., Yang, B., Liu, Y., Wang, Z., Ma, K., and Guan, X. Energy management based on multi-agent deep reinforcement learning for a multi-energy industrial park. *Applied Energy*, 311:118636, 2022. ISSN 0306-2619. doi: 10.1016/j.apenergy.2022.118636. URL <http://arxiv.org/pdf/2202.03771.pdf>.

A. Further Environment Details

The replayed data was mainly recorded or simulated in the time from 07.01.2007 to 28.12.2008. Although some episodes had to be left out due to missing data, there were more than 100 episodes, of which 95 were supposed to be used for training, 4 for testing and the rest for evaluation. The power was standardized to kilowatts, while the energy was simply kWh or kJ depending on the resolution. However, as the time steps are equidistant, power and energy can be modeled equivalently, since the power was assumed to be constant over the time step. Only some constants had to be adapted. The location of the house was in France near Paris.

The carbon intensity data was only available from 2021 and 2022 for France, so the carbon intensity might be biased, since the electricity mix might have drifted over the years. However, the daily, weekly and yearly frequencies should still be captured, although potentially drifted. The unit of carbon intensity is gram of CO₂ equivalent emissions per kWh or kJmin.

To prevent the ESS from overcharging or overdischarging, the rates were further constrained by the current charge and capacity, such that actually $C_t \in [0, \min\{C_{max}, \frac{B_{max}-B_t+D_s}{\sqrt{\nu}}\}]$ and $D_t \in [0, \min\{D_{max}, (B_t - D_s)\sqrt{\nu}\}]$.

B. Thresholding Baseline

$$a_t = \begin{cases} \begin{bmatrix} 1 & [1]^H & \psi 0.1 \\ -1 & [0]^H & 0 \\ 0 & [0]^H & \psi 0.1 \end{bmatrix} & \text{if } I_t < \phi_1 \\ \begin{bmatrix} 1 & [1]^H & \psi 0.1 \\ -1 & [0]^H & 0 \\ 0 & [0]^H & \psi 0.1 \end{bmatrix} & \text{if } I_t > \phi_2 \\ \begin{bmatrix} 1 & [1]^H & \psi 0.1 \\ -1 & [0]^H & 0 \\ 0 & [0]^H & \psi 0.1 \end{bmatrix} & \text{else} \end{cases} \quad (13)$$

where ϕ_1 and ϕ_2 are the lower and upper threshold respectively, while $\psi = \text{sign}(T_t - \frac{T_{max}+T_{min}}{2})$. The parameters for the thresholding algorithm were $\psi_1 = 65$ and $\psi_2 = 85$.

C. SAC

SAC is a squashed Gaussian policy, that employs entropy regularization, which adds a bonus reward in each time step proportional to the current entropy of the policy in an aim to encourage exploration. Furthermore, two Q-functions are learned and their minimal estimate is used to update the policy. The objective function for SAC is:

$$\max_{\theta} \mathbb{E}_{s \sim \mathcal{D}, \xi \sim \mathcal{N}} \left[\min_{j=1,2} Q_{\phi_j}(s, \tilde{a}_{\theta}(s, \xi)) - \alpha H(\pi_{\theta} | s) \right] \quad (14)$$

where θ denotes the policy parameter, ξ normal Gaussian noise, $\tilde{a}_{\theta}(s, \xi)$ the action sampled from the current policy, α the entropy regularization coefficient, and $H(\pi_{\theta} | s) = \log \pi_{\theta}(\tilde{a}_{\theta}(s, \xi) | s)$ the entropy of the policy. The action samples are obtained as $\tilde{a}_{\theta}(s, \xi) = \tanh(\mu_{\theta}(s) + \sigma_{\theta}(s) \odot \xi)$

D. PPO

PPO is a trust-region based policy gradient method, which solves a constrained policy update policy via SGD. It achieves the trust region remarkably simple, by employing the following update objective:

$$\theta_{k+1} = \arg \max_{\theta} \mathbb{E}_{s \sim \mathcal{D}, a \sim \pi_{\theta_k}} [L(s, a)] \quad (15)$$

$$L(s, a) = \min \left(\left| \frac{\pi_{\theta}(a | s)}{\pi_{\theta_k}(a | s)} \right|, 1 \pm \epsilon \right) A^{\pi_{\theta_k}}(s, a) \quad (16)$$

where $A^{\pi_{\theta_k}}(s, a)$ is the advantage of the current policy, and ϵ the trust region hyperparameter, clipping the update size. Alternatively, PPO can also be implemented using a KL-divergence constraint.

E. Training Procedure

All experiments were run for 250 episodes and in hourly resolution. Due to the encountered difficulty all were replaying only a single episode. Furthermore, the initial conditions, the initial indoor temperature T_0 , building mass temperature $T_{b,0}$, and initial charge B_0 , were fixed. The training parameters are shown in E.

Table 4. Training Parameters

PARAMETER	VALUE
B_{max}	13.5
C_{max}	1
D_{max}	1
ν	0.95
D_s	0.01
B_0	0
H	25
β	20
δ	5
T_0	20
$T_{b,0}$	20
r_a	0.04
r_b	0.1
r_h	0.05
q	0.05
L_{TCL}	5
T_{max}	23
T_{min}	18

F. Split Reward

$$r_{noise} = I_t(G_t - L_t) \quad (17)$$

$$r_{ESS} = I_t(D_t - C_t) \quad (18)$$

$$r_{FDR} = I_t\left(-\sum_{p \in U_e} p_r - \sum_{p \in U_d} \frac{2p}{H-1}\right) \quad (19)$$

$$r_{TCL} = I_t\left(-\frac{1}{r_h} L_{TCL} a_{tcl,t}\right) \quad (20)$$

$$r_{discomfort} = -\delta \exp\left(|T_t - \frac{T_{max} + T_{min}}{2}|\right) \quad (21)$$

The reward for TCL was split, since maintaining the temperature is a very different task than minimizing the energy consumption.